

The Inelastic Neutron Scattering Spectrum of $\text{H}_3\text{B:NH}_3$ and the Reproduction of Its Solid-State Features by Periodic DFT

Damian G. Allis, Mark E. Kosmowski, and Bruce S. Hudson*

Department of Chemistry, Syracuse University, Syracuse, New York 13244-4100

Received March 29, 2004; E-mail: bshudson@syr.edu

The borane–ammonia complex $\text{H}_3\text{B:NH}_3$ (borazane) is of interest because of the large (0.08 Å) decrease in the B:N bond length in the crystal compared to that of the vapor phase.¹ The polar dative B:N bond is similar to hydrogen bonding in specificity and thermal stability.² In the neutron diffraction structure the BH-to-NH hydrogen distances are (Figure 1) 2.02 Å (D2) and ca. 2.22 Å (D1 and D3), shorter than the 2.4 Å sum of their van der Waals radii and reflecting dihydrogen (di-H) bonding.³

The assignment of the B:N stretching mode and the origin of the B:N bond length change have been the source of much discussion. Theoretical studies have been performed to understand the origin of the structural change and to unambiguously identify the stretching mode in crystal and other condensed phases. A molecular cluster density functional theory (DFT) study determined that the dative bond length change results from strong dipole–dipole interactions.⁴ This argument is consistent with a dielectric model study that demonstrated that a solvent dipole field can affect the $\text{H}_3\text{B:NH}_3$ molecular structure as found in the solid.⁵ The cluster results also produce the di-H bonding interactions, but they do so in a cluster arrangement that does not correspond to the crystal molecular arrangement. In the application of a dielectric model to an ordered solid there arises an ambiguity because the molecules are not free to rotate. The measured dielectric constant of a solid formed by polar molecules is on the same order as that of a solid formed by nonpolar molecules. The $\text{H}_3\text{B:NH}_3$ internal mode and structural changes were also studied with *ab initio* methods by fixing $\text{H}_3\text{B:NH}_3$ positions to mimic the crystal arrangement around a single, unrestricted molecule.⁶ This study demonstrated the importance of the unit cell geometry on the electron density changes to $\text{H}_3\text{B:NH}_3$ and, therefore, the importance of the di-H bonds to the molecular properties in the solid. These results were used as a basis for the reassignment of a number of IR-active modes measured in a 2 K Ar matrix,⁷ KBr/Nujol,⁸ and liquid NH_3 .⁹

We report here the inelastic neutron scattering (INS) spectrum of crystalline $\text{H}_3\text{B:NH}_3$ to 1600 cm^{-1} and the results of periodic DFT calculations on the unit cell. The INS and DFT studies are employed together to assign the crystal normal modes of $\text{H}_3\text{B:NH}_3$ and to test the theoretical reproduction of the measured structural and vibrational changes. The intensities of an INS spectrum are dependent only on the extent of the hydrogen atom displacements along each normal mode coordinate. Accordingly, all INS and calculated modes are accessible for assignment and comparison in the reported region.

The INS experiment was carried out at the ISIS facility of the Rutherford Appleton Laboratory (Chilton, U.K.) using the time-focusing, crystal analyzer spectrometer TOSCA.¹⁰ A polycrystalline sample of ca. 2.9 g of $\text{H}_3\text{B:NH}_3$, obtained from Aldrich, was held at 30 K for this experiment. A description of neutron scattering, including results from TOSCA, is given in ref 11. The neutron diffraction crystallographic data for the 200 K unit cell² is as follows: Space group $Pmn2_1$, $a = 5.395(2)$ Å, $b = 4.887(2)$ Å, c

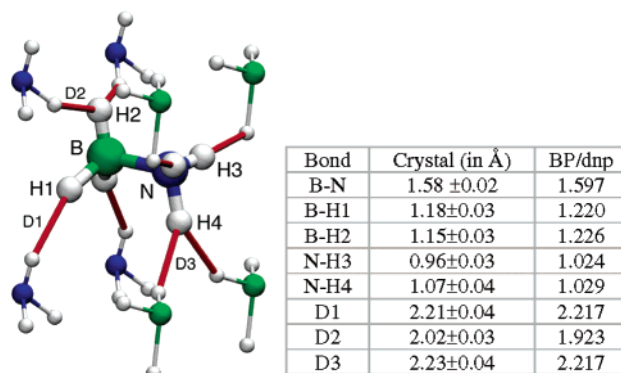


Figure 1. The $\text{H}_3\text{B:NH}_3$ molecule in its crystalline environment showing surrounding molecular fragments indicating di-H bonding (red). Graphics rendered with the program VMD.¹⁸

= 4.986(2) Å, $\alpha = \beta = \gamma = 90.0^\circ$, $Z = 2$. Isolated molecule and zone-centered ($k = 0$) periodic DFT geometry optimizations and normal mode calculations were performed with the BP functional¹² and dnp numerical basis set (BP/dnp) using DMol³¹³ on the SGI Origin Array at the National Center for Supercomputing Applications. Frequencies are unscaled.

Bond lengths and di-H bonding distances are provided in Figure 1. The BP/dnp isolated molecule (B:N = 1.666, B–H = 1.220, N–H = 1.022) calculations and microwave structure (B:N = 1.658, B–H = 1.216, N–H = 1.014)¹⁴ agree within 0.008 in all cases. The 0.06–0.10 B:N bond reduction in the crystal is 0.068 in the BP/dnp calculations. The calculated di-H distances are consistent with the actual unit cell within experimental error. The largest difference, D2, is a result of the apparent overestimation of the B–H2 bond length. The isolated C_{3v} molecular structure from the unit cell calculation lies 4.1 kJ/mol above the C_{3v} minimum energy structure in the BP/dnp calculation for the isolated molecule. The C_{3v} structure with the B:N length observed in the crystal lies 2.8 kJ/mol above the global minimum.

The $\text{H}_3\text{B:NH}_3$ INS, Ar matrix IR⁷ (frequencies only) and simulated molecular and solid-state BP/dnp spectra are provided from 50 to 1600 cm^{-1} in Figure 2. Excellent solid-state DFT agreement is observed with the fundamental modes of the INS spectrum through 1000 cm^{-1} . The overtone and combination INS bands above 1000 cm^{-1} can be identified on the basis of the INS/DFT fundamental mode assignments (Table 1). Of note is the prominence of the strong INS peaks at 202.4 cm^{-1} (phonon) and 333.7 cm^{-1} (B:N torsion) as combination bands with the B:N rocking modes at 1075 cm^{-1} (with 202.4 cm^{-1}) and the various BH_3 and NH_3 deformations at 1213/1231 and 1366/1423 cm^{-1} (with 333.7 cm^{-1}). Table 1 includes the BP/dnp isolated molecule and unit cell vibrations associated with the INS modes and their assignments. The complex nature of the INS spectrum at higher

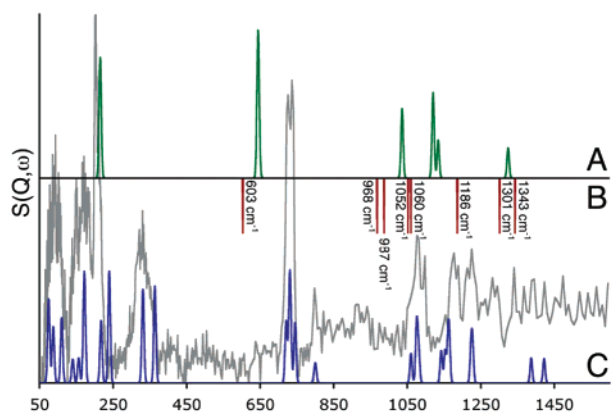


Figure 2. The 50–1600 cm^{-1} INS (gray), BP/dnp molecular (A), Ar matrix IR (only positions, B), and BP/dnp unit cell (C) spectra of $\text{H}_3\text{B:NH}_3$.

Table 1. $\text{H}_3\text{B:NH}_3$ Fundamental (Left) and Overtone and Combination Band (Right) Mode Assignments^a

Fundamental Mode Assignments			Identified Overtones and Combination Bands	
Isolated BP/dnp ^b	INS	Unit Cell BP/dnp ^c	cm^{-1}	assignment
		75.2	398.9	2(202.4)
		93.5	504.3	170.9 + 333.7
		110.5	660.2	2(333.7)
	150.1	140.5	822.2	725.8 + 93.5
		156.7	838.8	2(333.7) + 170.9
	170.9	171.4	872.9	725.8 + 150.1
		173.1	908.5	736.8 + 170.9
	202.4	217.5	917.6	822.2 + 93.5
		239.8	940.7	736.8 + 202.4
215.2 A2 torsion	333.7	331.4	1250.1	1049.8 + 202.4
644.3 E	725.8	720.7	1281.6	1076.3 + 202.4
NH_3 rock	736.8	729.8	1294.5	1098.0 + 202.4
		732.2, 745	1340.5	1189.3 + 150.1
			1395.0	1231.2 + 170.9
648.1 A1 B:N stretch	798.0	798.7	1451.8	2(725.8)
		801.1	1473.7	2(736.8)
1036.0 E	1049.8	1060.0	1488.5	1294.5 + 202.4
BH_3 rock	1076.3	1075.4	1518.5	1189.3 + 333.7
	1098.0	1076.1	1541.4	1213.2 + 333.7
		1081.4	1564.6	1231.5 + 333.7
1120.3 E	1177.4	1161.2	1580.3	1250.1 + 333.7
BH_3 scissor	1189.3	1164.2		
	1213.2	1223.8		
	1231.5	1227.7		
1134.2 A1	1154.2	1142.4		
BH_3 def.		1153.0		
1324.2 A1	1367.5	1387.0		
NH_3 def.	1423.2	1422.1		

^a Calculated fundamental assignments are grouped with their closest INS peaks. ^b Isolated molecule BP/dnp modes are provided with their symmetry assignments and relative motions. ^c Different grouped mode frequencies are the result of in-phase and out-of-phase combinations of the two $\text{H}_3\text{B:NH}_3$ in the unit cell.

energies is due to the contributions of combinations and overtones including phonon wings. These can be computed with the program aCLIMAX.¹⁵

Some disagreement exists between the Ar matrix and isolated $\text{H}_3\text{B:NH}_3$ calculated frequencies. The calculated modes and assignments are consistent with previous theoretical work. The gas-phase BP/dnp modes and those at the MP2/aug-cc-VDZ level of theory are within 0.7–6.1% of one another (MP2 error range: 0.07–8.1%; BP/dnp error range: 1.4–12.8%).¹⁶ Despite the absence of extended basis functions for DMol³, the BP/dnp results

provide excellent structural agreement with the microwave data. Differences in observed and calculated IR frequencies for high level (MP2) calculations have been ascribed to anharmonicity¹⁶ but could be due to matrix effects.

The significant B:N stretching mode shift is reproduced in the calculated spectrum with excellent agreement to an INS peak at 800 cm^{-1} , consistent with assignments in KBr/Nujol ($776/790 \text{ cm}^{-1}$) and liquid NH_3 (787 cm^{-1}). This mode was initially assigned to a pair of peaks at $968/987 \text{ cm}^{-1}$ in the Ar matrix (because of ¹⁰B and ¹¹B isotopes) but was reassigned, on the basis of the calculated frequency of 713 cm^{-1} in the *ab initio* study,⁶ as either unobserved or as a prominent peak at 603 cm^{-1} . As the only peak in the vicinity, the 603 cm^{-1} peak agrees best with the isolated molecule BP/dnp B:N stretching mode at 648 cm^{-1} . The B:N stretches in the crystal and the Ar matrix are expected to differ because the matrix B:N bond should have the longer length of the vapor. The shrinkage of the B:N bond in the crystalline solid is likely due to the formation of the di-H bonding network or a general intermolecular electrostatic effect, features that cannot occur in the Ar matrix. While the low-temperature Ar matrix IR spectrum would otherwise be an excellent foil for confirming the assignments of the INS/DFT spectra, it is clear from the comparison of the IR and INS spectra that the matrix and $\text{H}_3\text{B:NH}_3$ crystal are two very different environments. The large structural change observed for borazane is not unique but is rather common to dative bonded structures.^{1,17} A solvent model has been applied to sulfamic acid, which has the $\text{H}_3\text{N:SO}_3$ structure in the crystal.¹⁷

Acknowledgment. The ISIS Facility of the Rutherford Appleton Laboratory is thanked for access to TOSCA. This work was supported by U.S. National Science Foundation Grant CHE 0240104 and by the U.S. Department of Energy Grant DE-FG02-01ER14245. NCSA is thanked for SGI Origin Array access for the DMol³ calculations.

References

- (1) Leopold, K. R.; Canagaratna, M.; Phillips, J. A. *Acc. Chem. Res.* **1997**, *30*, 57.
- (2) Allis D. G.; Spencer J. T. Nanostructural Architectures from Molecular Building Blocks. In *Handbook of Nanoscience, Engineering, and Technology*; Goddard, W. A., III, Lyshevski, S. E., Brenner, D. W., Iarfrate, G. J., Eds.; CRC Press: Boca Raton, FL, 2002.
- (3) Klooster, W. T.; Koetzle, T. F.; Stegbahn, P. E. M.; Richardson, T. B.; Crabtree, R. H. *J. Am. Chem. Soc.* **1999**, *121*, 6337.
- (4) Merino, G.; Bakhmutov, V. I.; Vela, A. *J. Phys. Chem.* **2002**, *37*, 8491.
- (5) Bhl, M.; Steinke, T.; Schleyer, P. v. R. *Angew. Chem., Int. Ed. Engl.* **1991**, *30*, 1160. A second excellent discussion on the topic is provided in Jiao, H.; Schleyer, P. v. R. *J. Am. Chem. Soc.* **1994**, *116*, 7429.
- (6) Dillen, J.; Verhoeven, P. *J. Phys. Chem. A* **2003**, *107*, 2570.
- (7) Smith, L.; Seshadri, K. S.; White, D. *J. Mol. Spectrosc.* **1973**, *45*, 327.
- (8) Sawodny, W.; Goubeau, J. *Z. Phys. Chem.* **1965**, *44*, 227.
- (9) Taylor, R. C. *Adv. Chem. Ser.* **1964**, *42*, 59.
- (10) Colognesi, D.; Celli, M.; Cilloco, F.; Newport, R. J.; Parker, S. F.; Rossi-Albertini, V.; Sacchetti, F.; Tomkinson, J.; Zoppi, M. *Appl. Phys. A* **2002**, *74* (Suppl., Pt. 1), S64.
- (11) Hudson, B. S. *J. Phys. Chem. A* **2001**, *105*, 3949.
- (12) The BP functional. (a) Perdew, J. P.; Wang, Y. *Phys. Rev.* **1992**, *B45*, 13244. (b) Becke, A. D. *J. Chem. Phys.* **1988**, *88*, 2547.
- (13) Delley, B. *J. Chem. Phys.* **1990**, *92*, 508.
- (14) Thorne, L. R.; Suenram, R. D.; Lovas, F. J. *J. Chem. Phys.* **1983**, *78*, 167.
- (15) Ramirez-Cuesta, A. J. *Comput. Phys. Commun.* **2004**, *157*, 226. aCLIMAX is available at the ISIS Instrument and Support Web site. <http://www.isis.rl.ac.uk/molecularSpectroscopy/>.
- (16) Jagielska, A.; Moszynski, R.; Piela, L. *J. Chem. Phys.* **1999**, *110*, 947.
- (17) (a) Wong, M. W.; Wiberg, K. B.; Frisch, M. J. *J. Am. Chem. Soc.* **1992**, *114*, 523. (b) X-ray and neutron diffraction data can be found in: Bats, J. W.; Coppens, P.; Koetzle, T. F. *Acta Cryst.* **1977**, *B33*, 37.
- (18) Visual Molecular Dynamics (VMD). Humphrey, W.; Dalke, A.; Schulten, K. *J. Mol. Graphics* **1996**, *14*, 33.

JA048215M